High-Pulse-Energy Mid-Infrared Fractional-Image-Rotation-Enhancement $ZnGeP_2$ Optical Parametric Oscillator

Marc Eichhorn,[1,*] Martin Schellhorn,[1] Magnus W. Haakestad,[2] Helge Fonnum,[2] and Espen Lippert[2]

[1]*French-German Research Institute of Saint-Louis (ISL), 5 rue du Général Cassagnou, 68301 Saint-Louis Cedex, France*
[2]*Norwegian Defense Research Establishment (FFI), P.O. Box 25, NO-2027, Kjeller, Norway*
**Corresponding author: marc.eichhorn@isl.eu*

Received XX Month XXXX; revised XX Month, XXXX; accepted XX Month XXXX; posted XX Month XXXX (Doc. ID XXXXX); published XX Month XXXX

A high-energy mid-infrared $ZnGeP_2$ (ZGP) optical parametric oscillator (OPO) based on the non-planar Fractional- Image- Rotation- Enhancement (FIRE) resonator pumped by a 2.05 µm Ho^{3+}:YLF laser is presented. Up to 120 mJ pulse energy in a rotationally symmetric beam is generated in the 3-5 µm wavelength range at 1 Hz repetition rate. Slope efficiencies of up to 78 % are achieved with respect to the pump pulse energy incident onto the ZGP crystal. The OPO pulses have duration close to 15 ns, corresponding to a maximum peak power of 8 MW. A measurement of M^2 dependence on pump beam diameter is presented. © 2016 Optical Society of America

OCIS codes: *(190.4360) Nonlinear optics, devices; (190.4970) Parametric oscillators and amplifiers.*

http://dx.doi.org/10.1364/OL.99.099999

Non-linear conversion in optical parametric oscillators (OPOs) from the 2 µm to the mid-infrared (3–7 µm) range is of rapidly increasing interest for applications in long-range detection, medicine and countermeasures, with a strong trend towards high pulse energies and average powers, where substantial progress has been achieved in recent years [1–6]. In high-energy nanosecond pulse systems, the main challenge is to maintain good beam quality while increasing the energy. This is because the beam diameter has to be increased in order to stay below the damage threshold of the nonlinear medium, leading to high Fresnel number of the resonator and thereby poor mode discrimination. This problem can be solved by using a master oscillator-power amplifier (MOPA) system, where the output from a low-energy and good-beam-quality OPO is amplified without significant degradation of the beam quality. However, MOPA systems tend to be relatively complex, so it is of interest to study the performance limitations of simple OPOs. In principle, the mode discrimination of the OPO could be improved by increasing the OPO resonator length, but this would lead to reduced efficiency due to a longer signal build-up time, and would also result in increased system size. Another possibility is to use image rotation in a non-planar ring cavity, such as the RISTRA [7] or FIRE [8] resonator. Such resonators require the use of critical phase matching, with significant transverse walk-off between the signal and idler in the critical plane, in order to improve beam quality substantially. This is not the case in most mid-infrared OPOs using collinearly type I phase-matched $ZnGeP_2$ (ZGP) as the nonlinear material. Nevertheless, FIRE resonators are still attractive because they provide a rotationally symmetric output beam, and such a resonator has been used in the present study of a mid-infrared ZGP OPO pumped by a 2.05 µm Ho^{3+}:YLF laser. We study the dependence of the beam quality and achievable pulse energy on the pump beam diameter, and obtain a record high output energy of 120 mJ in the 3-5 µm wavelength range from a mid-infrared OPO, as well as slope conversion efficiencies of up to 78 %.

The experimental setup is shown in Fig. 1. It consists of a cryogenically-cooled Ho^{3+}:YLF pump laser [9], a telescopic relay-imaging system realized by the lenses L1 and L2, which images a plane close to the pump laser output coupler onto the OPO crystal entrance face, a vacuum tube VT to avoid air breakdown in the intermediate focus of the relay-imaging telescope and the FIRE OPO. The Ho^{3+}:YLF pump laser delivers 18 ns long pulses with a pulse energy of up to 0.5 J at a wavelength of 2.05 µm at 1 Hz repetition rate, and has a beam quality M^2 = 1.5. It produces an approximately flat wave front at the output, and for optimum conversion efficiency the beam is relay imaged onto the OPO crystal. Three different focal lengths of the lens L2 are used to generate collimated pump beam diameters (FWe-^{2}M) of 2.6 mm, 5.5 mm and 8.6 mm, respectively, at the position of the OPO crystal. A half-wave plate and a polarizer allow for attenuating the pump energy without altering pulse duration and pump beam profile. Taking into account the total transmission of the pump beam-forming optics, the maximum pump energy incident onto the OPO crystal entrance face available for the experiments is 320 mJ. To obtain enough parametric gain two 14 x 12 x 6 mm^3 $ZnGeP_2$ crystals cut for

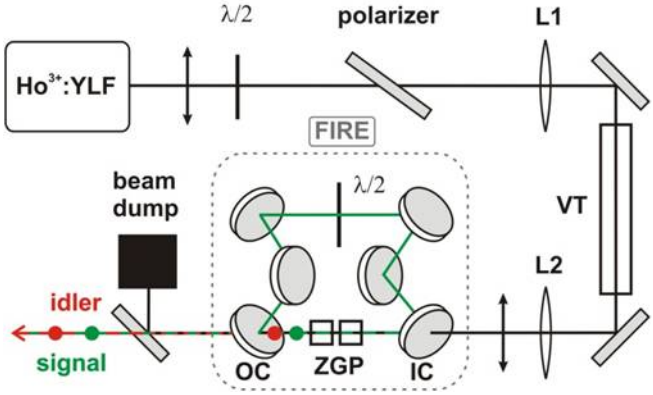

Fig. 1. Schematic outline of the FIRE ZGP OPO setup.

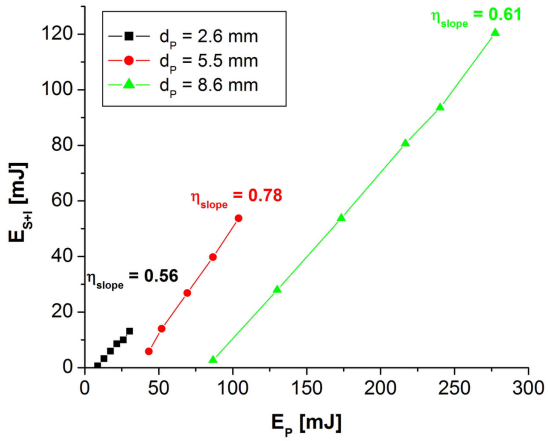

Fig. 2. OPO output pulse energy (sum of signal and idler) vs. incident pump pulse energy.

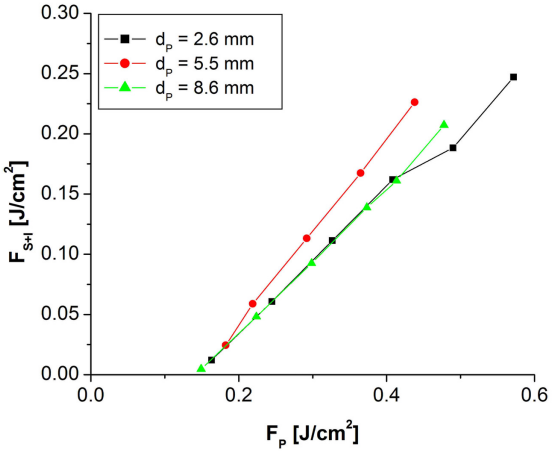

Fig. 3. OPO output beam average fluence (sum of signal and idler) vs. incident pump average fluence for different pump spot diameters.

type-I phase matching (θ = 54°) are employed in series, mounted into the same crystal holder. Before the experiments, the crystal holder is transversely centered on the pump beam and adjusted in phase-matching angle for maximum OPO output pulse energy, resulting in a signal wavelength around 3.7 µm and an idler around 4.6 µm. The FIRE resonator consists of six mirrors in a non-planar arrangement, providing a fractional image rotation per round trip, whose angle is chosen in such a way that a large number (theoretically an infinite number) of round-trips would be necessary to re-establish image self-consistency [8]. The incident angle for the resonating signal on all six mirrors is 32.7°, identical to the corresponding incidence angle in a RISTRA cavity. The output coupler OC of the FIRE resonator has a reflectivity of 65 % for the signal and high transmission for the pump (T > 95 %) and idler (T > 98 %) wavelengths. The input coupler and the other four mirrors are identical and have high transmission for the pump (T = 86.7 %) and idler (T > 94 %) and are highly reflective for the signal (R > 99 %). The total round-trip image rotation is 77.45°. As a result, 14 round-trips are needed before the original transverse image is essentially restored (total rotation angle = 3 x 360° + 4.3°). The length of the FIRE cavity is *L*=222 mm. The residual pump after the OPO is filtered out by a

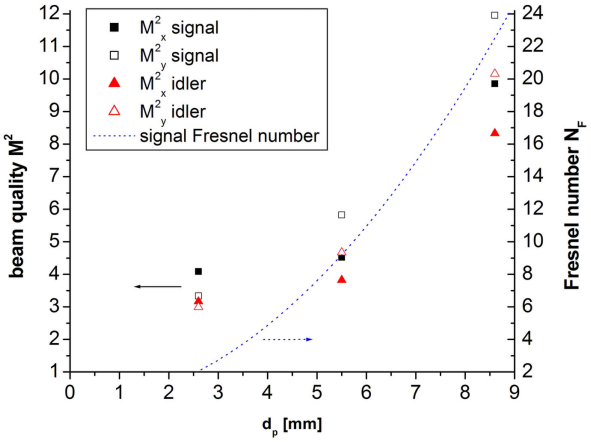

Fig. 4. OPO beam quality and signal Fresnel number vs. pump spot diameter measured at maximum pump energy in Fig. 2.

dichroic mirror highly reflective (R > 99 %) for the pump and highly transmitting for signal and idler (T = 93 %). All measured OPO output values are corrected for these transmission losses.

As depicted in Fig. 2 the OPO threshold increases with increasing pump spot diameter from 6.3 mJ at 2.6 mm pump spot over 34 mJ at 5.5 mm pump spot to 82 mJ at 8.6 mm pump spot diameter. To avoid crystal damage, the highest peak fluence allowed in the experiments is set to 1 J/cm^2. Under these conditions, maximum fluence-limited output pulse energies (signal and idler together) of 13.1 mJ, 53.8 mJ and 120.4 mJ are reached with slope efficiencies of 56 %, 78 % and 61 % for the three pump spot sizes, respectively. No readjustment of the phase-matching angular orientation of the ZGP crystal holder was necessary for the different pump spot sizes in order to obtain maximum output energy in each case.

Rescaling the pump and output energy to the corresponding average fluence $F = E / (\pi d_p^2/4)$ gives comparable results in output fluence, as can be seen in Fig. 3. The pump threshold fluence is approximately 0.14 J/cm^2 in all cases. The slope, however, is remarkably higher for the 5.5 mm pump spot size compared to the pump beam diameters of 2.6 mm and 8.6 mm. The reason for this could stem from a flatter and thus more adapted wave front of the 5.5 mm diameter pump beam compared to the 2.6 mm diameter pump beam due to aberrations from the relay imaging optics, which are assumed to be stronger in the 2.6 mm case owing to the shorter focal length of L2 involved. For the 8.6 mm diameter pump beam and the associated larger resonant signal beam additional losses due to clipping by the ZGP crystal apertures may occur, which may cause the decrease in slope for the larger pump spot size.

The M^2 beam propagation factor of the OPO output, shown in Fig. 4, is determined separately along the transverse x- and y-axis by imaging the near and far field of the OPO output beam onto a PyroCam III camera, extracting the beam size and divergence, and calculating the corresponding M^2 value by

$$M^2 = \frac{\pi}{\lambda}\theta w_m, \qquad (1)$$

where w_m is the waist radius of the beam profile and θ its divergence half angle, calculated from the second moments of the measured beam profiles. Also depicted is the effective Fresnel number calculated from the pump spot diameter as limiting aperture,

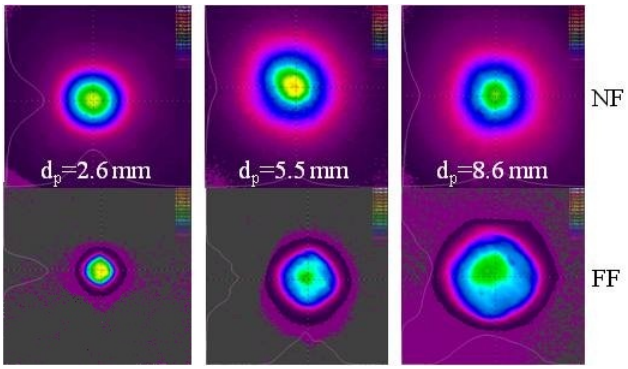

Fig. 5. OPO output beam profile (signal + idler) at maximum pump energy for each pump spot diameter indicated (top: near field at OPO exit, bottom: far field after transformation by a lens) .

$$N_F = \frac{d_p^2}{4\lambda_s L}, \qquad (2)$$

with λ_s being the signal wavelength and L the FIRE cavity round-trip length. The value of the M^2 parameter increases with increasing pump spot size, as can be seen in Fig. 4. At the smallest pump spot diameter, the effective Fresnel number is close to 2, which is not sufficiently small to obtain a diffraction-limited (M^2 = 1) signal and idler beam. A constant beam divergence would imply a beam quality proportional to the pump diameter, assuming a signal and idler diameter proportional to the pump diameter. However, such a linear relationship is not observed in Fig. 4 . Owing to the low repetition rate of 1 Hz the incident average power even at maximum pump energy is around 270 mW, from which only a small amount is converted into heat by the residual crystal absorption at the pump wavelength. It can thus be assumed that no thermal lens occurs in the ZGP crystals.

The emitted OPO beam near field and far field profiles are depicted in Fig. 5 for the highest pulse energy for each of the pump spot diameter curves shown in Fig. 2. It can be seen that the profiles are highly rotationally symmetric as expected from the fractional image rotation of the FIRE cavity.

The temporal pulse shape at the maximum output energy of 120 mJ at 8.6 mm pump spot diameter was measured with a VIGO detector with a nominal time constant below 1 ns. The oscilloscope traces obtained are shown in Fig. 6 for the OPO output, the incident and the depleted pump pulse. The depleted pump pulse and the OPO pulse therein are scaled and shifted in time in order to correct for the different time delays and intensity variations due to different pick-up positions of the photodetector used. The temporal region in which efficient conversion takes place can be seen in the depleted pump pulse as a plateau at the end of the pulse. Here, however, due to the short pulse width this plateau is less pronounced than in ZGP OPOs pumped with longer pulses [10]. Normalizing the pulse trace by its time integral and multiplying it with the pulse energy yields the temporal pulse power trace shown in the inset of Fig. 6. The highest pulse energy achieved at 8.6 mm pump spot diameter corresponds to an estimated maximum peak power of 8 MW.

The duration (FWHM) of the generated pulses increases from around 11 ns at threshold to around 15 ns for fluences around 0.5 J/cm^2, as can be seen in Fig. 7. We observe that the pulses in the case of the 5.5 mm pump spot size are longer than in the other two cases, showing that for the 5.5 mm pump spot the OPO build-up time is shorter. Therefore, in this case the nonlinear gain is higher than the one created for the 2.6 mm or the 8.6 mm pump beam diameter at identical average fluence. This reduces the signal build-up time which results in a higher conversion efficiency.

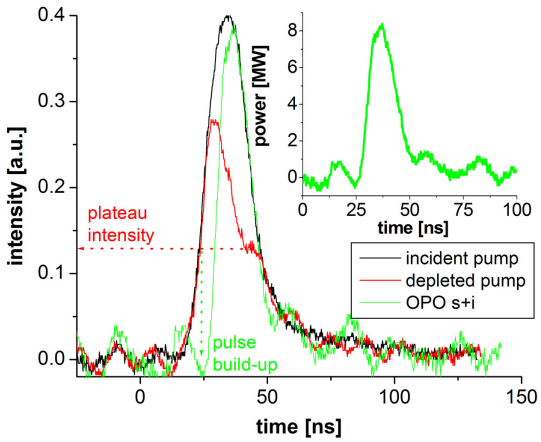

Fig. 6. Pulse shape of incident and depleted pump and OPO output pulse vs. time at an output energy of 120.4 mJ. The inset shows the temporal OPO output power of the pulse vs. time.

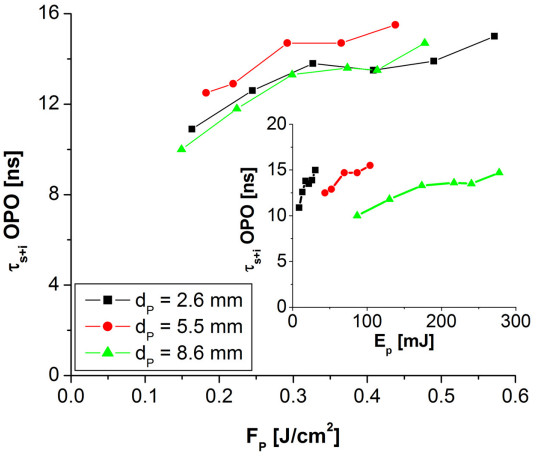

Fig. 7. Pulse duration [FWHM] of the OPO output pulses vs. pump fluence. The inset shows the pulse duration vs pump energy.

In conclusion, an efficient high-energy mid-infrared $ZnGeP_2$ OPO based on the non-planar FIRE resonator pumped by a 2.05 µm Ho^{3+}:YLF laser has been demonstrated. Up to 120 mJ of mid-infrared pulse energy in the 3-5 µm wavelength range is generated at 1 Hz repetition rate. Slope efficiencies of up to 78 % are achieved with respect to the pump pulse energy incident onto the ZGP crystal. The beam profiles generated from the FIRE cavity are highly rotationally symmetric. The OPO pulses have a duration of about 15 ns, corresponding to a maximum peak power of 8 MW.

References

1. A. Dergachev, D. Armstrong, A. Smith, T. Drake, and M. Dubois, Opt. Express **15**, 14404–14413 (2007).
2. C. Kieleck, M. Eichhorn, A. Hirth, D. Faye, and E. Lallier, Opt. Lett. 34, 262–264 (2009).
3. E. Lippert, H. Fonnum, G. Arisholm, and K. Stenersen, Opt. Express 18, 26475-26483 (2010).
4. M. Eichhorn, G. Stoeppler, M. Schellhorn, K. T. Zawilski, and P. G. Schunemann, Appl. Phys. B 108, 109–115 (2012).

5. G. Stöppler, M. Schellhorn, and M. Eichhorn, Laser Physics 22, 1095-1098 (2012).
6. M. W. Haakestad, H. Fonnum, and E. Lippert, Opt. Express 22(7): 8556-64 (2014).
7. A. V. Smith and D. J. Armstrong, J. Opt. Soc. Am. B 19, 1801–1814 (2002).
8. S. Bigotta, G. Stöppler, J. Schöner, M. Schellhorn, and M. Eichhorn, Opt. Mat. Ex. 4 (3), 411-423 (2014).
9. H. Fonnum, E. Lippert, and M.W. Haakestad, Opt. Lett. 38 (11), pp. 1884-1886 (2013).
10. C. Kieleck, M. Eichhorn, D. Faye, E. Lallier, S.D. Jackson, Proc. of SPIE Vol. 7582, 758212 (2010).

References with titles:

1. A. Dergachev, D. Armstrong, A. Smith, T. Drake, and M. Dubois, "3.4-µm ZGP RISTRA nanosecond optical parametric oscillator pumped by a 2.05-µm Ho:YLF MOPA system", Opt. Express **15**, 14404–14413 (2007).
2. C. Kieleck, M. Eichhorn, A. Hirth, D. Faye, and E. Lallier, "High-efficiency 20-50 kHz mid-infrared orientation-patterned GaAs optical parametric oscillator pumped by a 2 µm holmium laser", Opt. Lett. 34, 262–264 (2009).
3. E. Lippert, H. Fonnum, G. Arisholm, and K. Stenersen, "A 22-watt mid-infrared optical parametric oscillator with V-shaped 3-mirror ring resonator", Opt. Express 18, 26475-26483 (2010).
4. M. Eichhorn, G. Stoeppler, M. Schellhorn, K. T. Zawilski, and P. G. Schunemann, „Gaussian- versus flat-top pumping of a mid-IR ZGP RISTRA OPO", Appl. Phys. B 108, 109–115 (2012).
5. G. Stöppler, M. Schellhorn, and M. Eichhorn, „Enhanced beam quality for medical applications at 6.45 µm by using a RISTRA ZGP OPO", Laser Physics 22, 1095-1098 (2012).
6. M. W. Haakestad, H. Fonnum, and E. Lippert, "Mid-infrared source with 0.2 J pulse energy based on nonlinear conversion of Q-switched pulses in ZnGeP2", Opt. Express 22(7): 8556-64 (2014).
7. A. V. Smith and D. J. Armstrong, "Nanosecond optical parametric oscillator with 90° image rotation: design and performance", J. Opt. Soc. Am. B 19, 1801–1814 (2002).
8. S. Bigotta, G. Stöppler, J. Schöner, M. Schellhorn, and M. Eichhorn, „Novel non-planar ring cavity for enhanced beam quality in high-pulse-energy optical parametric oscillators", Opt. Mat. Ex. 4 (3), 411-423 (2014).
9. H. Fonnum, E. Lippert, and M.W. Haakestad, "550 mJ Q-switched cryogenic Ho:YLF oscillator pumped with a 100 W Tm:fiber laser", Opt. Lett. 38 (11), pp. 1884-1886 (2013).
10. C. Kieleck, M. Eichhorn, D. Faye, E. Lallier, S.D. Jackson, "Polarization effects and fiber-laser-pumping of a 2-µm-pumped OP-GaAs OPO", Proc. of SPIE Vol. 7582, 758212 (2010).